

1 **Revision 1 DFT simulation of the occurrences and correlation of gold**
2 **and arsenic in pyrite**

3 **JIAN-HUA CHEN^{1,2}, YU-QIONG LI^{2,*}, SHUI-PING ZHONG¹, JIN-GUO³**

4 ¹ Zijin Mining Group Co., Ltd., Longyan, Fujian province 364200, China

5 ² College of Resources and Metallurgy, Guangxi University, Daxue Road 100,
6 Nanning, Guangxi province 530004, China

7 ³ College of Physics Science and Engineering, Guangxi University, Daxue Road 100,
8 Nanning, Guangxi province 530004, China

9 **ABSTRACT**

10 Using density functional theory (DFT) calculations, the occurrences and
11 correlation of gold (Au) and arsenic (As) in pyrite were studied, and the effect of As
12 on the structural stability of Au in pyrite (FeS₂) was investigated. The calculated
13 results show that Fe is not likely to be simply substituted with Au under normal
14 circumstances. The presence of As is very conducive to incorporating Au into the
15 pyrite interstitial lattice site along with substitution for the S site. It is predicted that a
16 positive correlation exists between Au and As in pyrite and that the higher is the As
17 concentration, the more easily Au is formed in the pyrite. Additionally, with
18 increasing As content, the Fe site is occupied by the interstitial Au. The pyrite lattice
19 expands with the incorporation of Au and As. Antibonding interactions are found
20 between the Au, Fe and As atoms. The reducibility of pyrite is greatly enhanced due to
21 the presence of Au and As. The electronic structure calculations show that substituting

* E-mail: lyq198205@163.com

22 Au and As for S atoms does not change the pyrite p-type property and that defect
23 energy levels are present in the conduction band. However, with increasing As
24 concentration, incorporating the interstitial site of Au causes a change from the p-type
25 pyrite to an n-type pyrite, and defect energy levels are mainly located in the energy
26 band gap. The interstitial site of Au causes the pyrite to be spin-polarized at certain As
27 content. In addition, strong interactions are found between Fe 3d and Au 6p orbitals
28 and between Au 5d and As 4p orbitals.

29 **Key words:** pyrite; gold-arsenic; correlation; DFT calculation

30 INTRODUCTION

31 Gold (Au) and arsenic (As) are two common heterogeneous atoms that often
32 appear together in natural pyrite. It was suggested that a strong association exists
33 between As and Au in pyrite and that a large amount of invisible gold is present in
34 arsenic pyrite. In addition, gold was found to occur more in arsenic-rich pyrite than in
35 arsenic-poor pyrite. Moreover, strong positive correlations between the As and Au
36 content of pyrite were proposed (Wells and Mullens 1973; Cook and Chryssoulis
37 1990; Arehart et al. 1993; Fleet et al. 1993; Abraitis et al. 2004). Reich et al. (2003,
38 2005) studied the solubility of gold in arsenic pyrite and suggested a maximum Au/As
39 molar ratio of approximately 0.02.

40 It was suggested that arsenic could be present at the sulfur site in pyrite, resulting
41 in the formation of the AsS^{3-} dianions within the lattice (Blanchard et al. 2007;
42 Abraitis et al. (2004)), and our study has shown that Au would most likely exist in
43 pyrite incorporated into interstitial lattice sites and substituted for S atoms. Using

44 XANES measurements on gold-bearing arsenic pyrite, Simon et al. (1999) suggested
45 that the gold present as Au^{1+} was located in the arsenic pyrite lattice. In addition,
46 four-fold-coordinated Au^{1+} was more abundant than two-fold-coordinated forms.
47 However, the nature of four-fold-coordinated Au^{1+} is not well understood. Simon et
48 al. suggested that Au might be present as an Au-As-S compound, where gold would
49 be bonded in four-fold coordination as compared to sulfur and arsenic atoms or in
50 vacancy positions on a cation site in arsenic pyrite. In addition, they suggested that
51 Au^{1+} was most likely incorporated into arsenic pyrite by adsorption onto pyrite
52 surfaces during crystal growth. The coupled substitution mechanism was proposed to
53 explain the strong positive correlation between Au and As in pyrite (Arehart et al.
54 1993; Fleet et al. 1993). Their studies have clearly shown extensive oscillatory
55 zonation in both the Au and As contents of single pyrite grains. It was suggested that
56 the AsS^{3-} dianion may be charge compensated by Au^{3+} in the mineral lattice, i.e.,
57 Au^{3+} substitutes for Fe^{2+} and AsS^{3-} substitutes for the S_2^{2-} dianion. Simon et al.
58 (1999) suggested that the correlation between gold and arsenic might be related to
59 the role of arsenic in enhancing the adsorption of gold on the pyrite surface, possibly
60 through semiconductor effects.

61 Some studies on the mode of occurrence of gold and arsenic in pyrite have been
62 conducted; however, the crystal structure of pyrite bearing gold and arsenic and
63 whether there is a positive correlation between them are still not very clear. Moreover,
64 the detailed properties of Au- and As-bearing pyrite are not very well studied or
65 understood. In this study, using density functional theory (DFT) calculations, the

66 occurrences and correlation of Au and As in pyrite were studied; additionally, the
67 effect of As on the structural stability of Au in pyrite was investigated.

68 COMPUTATIONAL DETAILS

69 Based on density functional theory, all calculations were performed using
70 CASTEP, GGA-PW91 (Perdew et al. 1992). Only the valence electrons Fe $3d^6 4s^2$, S
71 $3s^2 3p^4$, As $4s^2 4p^3$ and Au $5d^{10} 6s^1$ were considered explicitly through the use of
72 ultrasoft pseudopotentials (Vanderbilt 1990). The effects of the supercell size on the
73 defect properties were investigated, and a $2 \times 2 \times 2$ pyrite supercell size ($Fe_{32}S_{64}$) is
74 sufficient to guarantee reliable calculation results. When a plane wave cut-off energy
75 of 270 eV was used, the calculated lattice parameter and band gap were 5.418 Å and
76 0.60 eV, respectively, compared to the experimental values of 5.417 Å (Prince et al.
77 2005) and 0.95 eV (Schlege and Wachter 1976). A Monkhorst-Pack (Monkhorst and
78 Pack 1976; Pack and Monkhorst 1977) k -point sampling density of $2 \times 2 \times 2$ was used.
79 The convergence tolerances for the geometry optimization calculations were set to a
80 maximum displacement of 0.002 Å, a maximum force of $0.08 \text{ eV} \cdot \text{Å}^{-1}$, a maximum
81 energy change of $2.0 \times 10^{-5} \text{ eV} \cdot \text{atom}^{-1}$ and a maximum stress of 0.1 GPa, and the
82 self-consistent field (SCF) convergence tolerance was set to $2.0 \times 10^{-6} \text{ eV} \cdot \text{atom}^{-1}$. In
83 addition, the spin calculation was performed during the simulation. It was indicated
84 that the calculation will be performed using different wavefunctions for different spins
85 (Hohenberg and Kohn 1964; Kohn and Sham 1965; Barth and Hedin 1972; Vosko et
86 al. 1980; Cocula et al. 2003).

87 The formation energy refers to the energy required for an Au (As) atom to

88 incorporate into the crystal. Here, the formation energy of a site-defect element in the
89 pyrite lattice, ΔE , is defined as follows (Nishidate et al. 2008):

$$90 \quad \Delta E = E_{product}^{total} + E_x - E_{reactant}^{total} - E_{Au(As)}$$

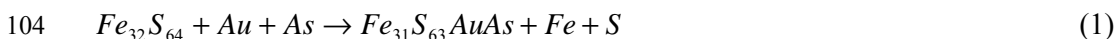
91 where $E_{product}^{total}$ and $E_{reactant}^{total}$ are the total energies of those pyrites bearing As and/or
92 Au and perfect pyrites, respectively. E_x and $E_{Au(As)}$ are defined as the calculated
93 total energies of the substituted matrix atom ($x = \text{Fe}$ or S) and the Au or As atom, i.e.,
94 the pseudo atomic energy, which is calculated during the optimized cell process. The
95 smaller is the value of ΔE , the more likely it is that the element exists in pyrite.

96

97 **CORRELATION OF AU AND AS IN PYRITE**

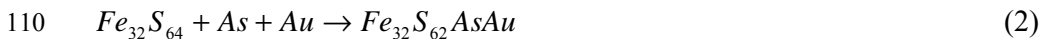
98 Our studies have shown that gold (Au) would most likely exist in the pyrite
99 crystal at the interstitial lattice sites and through substitution for S atoms, and As
100 substituting for S was the most energetically favored mechanism (Savage et al. 2000;
101 Blanchard et al. 2007).. In this study, Au substituting for Fe in pyrite under the effect
102 of As was investigated. This reaction is shown as follows:

103 One Au substituting for one Fe and one As substituting for one S:

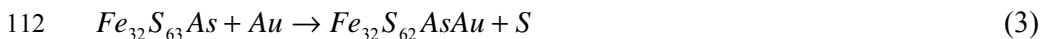


105 Reactions (2)-(4) describe the substitution of Au for S in pyrite with increasing
106 As concentration, and reactions (5)-(9) describe the Au at interstitial sites in pyrite
107 under the As mass concentrations of 0.0%, 1.93%, 3.82%, 5.67% and 7.48%,
108 respectively.

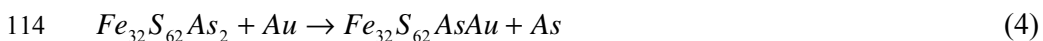
109 One As and one Au substituting for one S_2 unit at the same time:



111 One Au substituting for the S of the AsS unit:



113 One Au substituting for one As of the As₂ unit:



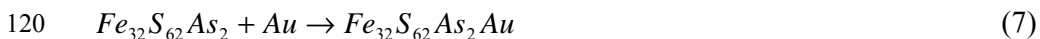
115 One Au incorporating into the interstitial site of Fe₃₂S₆₄:



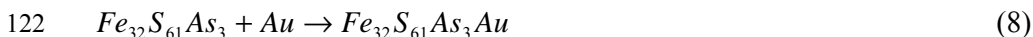
117 One Au incorporating into the interstitial site of Fe₃₂S₆₄ substituted by one As atom:



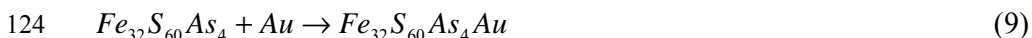
119 One Au incorporating into the interstitial site of Fe₃₂S₆₄ substituted by two As atoms:



121 One Au incorporating into the interstitial site of Fe₃₂S₆₄ substituted by three As atoms:



123 One Au incorporating into the interstitial site of Fe₃₂S₆₄ substituted by four As atoms:



125 The calculated formation energies for reactions (1)-(9) are shown in Table 1.

126 The formation energies of Au substituting for Fe (reaction (1)), Au substituting for S

127 (reaction (2)) and Au incorporating into the interstitial site (reaction (5)) are 10.97,

128 4.62 and 5.89 eV, respectively. This result suggests that reaction (1) is difficult to

129 undergo, indicating that it is almost impossible for Fe to be substituted simply by Au

130 under normal circumstances. For reactions (2) to (4), the formation energies of Au

131 substituting for S decrease with increasing As concentration. This result indicates that

132 the reactions are promoted due to the presence of As. In addition, comparing reactions
133 (3) and (4) show that the reaction of Au substituting for As (reaction (4)) is more
134 likely to occur than the reaction of Au substituting for S (reaction (3)), which suggests
135 that the presence of As was conducive to the incorporation of Au. When Au is
136 incorporated at interstitial sites (reactions (5)-(9)), it is shown that the formation
137 energy is significantly lowered from +5.89 eV to +0.67 eV, with an increasing As
138 concentration of 0% to 7.48%, suggesting that the reactions are promoted as the As
139 concentration increased.

140 The formation energy calculation results show that the presence of As is very
141 conducive to the incorporation of Au into pyrite, regardless of whether the Au is in the
142 S site or interstitial site, and it can be concluded that a positive correlation exists
143 between Au and As in pyrite. In addition, it is noted that the formation energies of
144 reactions (8) and (9) are obviously low compared to other reactions, which suggests
145 that such highly concentrated As bearing structures are very favorable for the
146 incorporation of Au into pyrite.

147 **CRYSTAL STRUCTURE OF PYRITE CONTAINING AU AND AS**

148 Fig. 1 and 2 show the reacting processes of (2)-(9). It can be observed from Fig.
149 1 that the incorporation of Au and As into the S site has a small influence on the
150 internal structure of the pyrite crystal, and the structures of their surrounding Fe and S
151 atoms are not influenced. This result suggests that the pyrite structure would be stable
152 when Au and As are introduced into S sites.

153 The pyrite crystal structure with Au at an interstitial site is shown in Fig. 2. It is

154 shown that the structure of pyrite with an interstitial Au at an As concentration of
155 1.93% ($\text{Fe}_{32}\text{S}_{63}\text{AsAu}$) was similar to that of pyrite at an As concentration of 0%
156 ($\text{Fe}_{32}\text{S}_{64}\text{Au}$). However, the pyrite structure is significantly changed with a further
157 increase in the As concentration. It is clearly shown that the Fe1 atom (in the vicinity
158 of Au) in $\text{Fe}_{32}\text{S}_{62}\text{As}_2\text{Au}$, $\text{Fe}_{32}\text{S}_{61}\text{As}_3\text{Au}$ and $\text{Fe}_{32}\text{S}_{60}\text{As}_4\text{Au}$ is repelled into the hole due
159 to the incorporation of Au, and its original position is occupied by Au. These results
160 suggest that Au may exist in pyrite by substituting for Fe at a high As content.

161 The cell lengths and angles of pyrite containing Au and As were investigated, as
162 shown in Table 2. The incorporation of Au and As into S sites ($\text{Fe}_{32}\text{S}_{62}\text{AuAs}$) results
163 in a small pyrite lattice expansion, and the expansion rate is only of 0.34%, while the
164 incorporation of interstitial Au lead to a great deformation of the lattice, and the
165 expansion rate is greater than 1%. In addition, the degree of changes in angles of
166 pyrite cell is different due to the different incorporation behavior of Au. The
167 interstitial Au results in a greater degree of changes in crystal angles than the
168 substituting Au. Moreover, the degree of deformation increases with the increase in As
169 content. This result is related to the covalent radii of the atoms (Au (1.34 Å), As (1.21
170 Å), Fe (1.17 Å) and S (1.02 Å)).

171 The Mulliken overlap population of bonds may be used to assess the bonding and
172 antibonding states between atoms and positive and negative values indicate bonding
173 and antibonding states, respectively (Segall et al. 1996). The calculated results listed
174 in Table 3 show that the Au atoms are bonded to Fe and As atoms and are present in
175 an antibonding state in the pyrite. The bond populations between As-Au and Fe-Au

176 bonds are stronger in $\text{Fe}_{32}\text{S}_{62}\text{AsAu}$ and $\text{Fe}_{32}\text{S}_{63}\text{AsAu}$ than in $\text{Fe}_{32}\text{S}_{62}\text{As}_2\text{Au}$,
177 $\text{Fe}_{32}\text{S}_{61}\text{As}_3\text{Au}$ and $\text{Fe}_{32}\text{S}_{60}\text{As}_4\text{Au}$, suggesting that the antibonding interactions between
178 atoms in the former are greater than in the latter. In addition, for the case of interstitial
179 Au, the antibonding interaction between the Fe and Au atoms is weakened with
180 increases in the As content, while the antibonding interaction between As and Au is
181 not changed significantly.

182 By analyzing the atomic charge using the charge equilibration (QEq) method, it
183 is shown that As is positively charged in the pyrite. The positive charges on the Fe
184 atoms are lowered due to the incorporation of As. In addition, the positive charges on
185 the Fe and As atoms decrease with increases in the As concentration. These results
186 suggest that the presence of As could enhance the reducibility of the pyrite. After
187 incorporating Au into the crystal, the positive charges on Fe and As are further
188 reduced as the As concentration increases, and the positive charge on the Au atom
189 itself also decreases. The reducibility of pyrite is apparently greatly enhanced due to
190 the presence of Au and As.

191

192 **ELECTRONIC STRUCTURES OF PYRITE-BEARING AU AND AS**

193 The electronic structures of pyrite would be significantly influenced due to the
194 incorporation of Au and As. The band structures of perfect and Au- and As-bearing
195 pyrites are shown in Fig. 3 (the zero point of the energy was set at the Fermi level, E_F).
196 The substitution of Au and As for S atoms ($\text{Fe}_{32}\text{S}_{62}\text{AsAu}$) do not change the p-type
197 property of the pyrite, and defect energy levels are present in the conduction band.

198 However, with increasing As concentration, the incorporation of Au at an interstitial
199 site change the p-type pyrite to an n-type pyrite, and defect energy levels are mainly
200 located in the energy band gap. In addition, Fig. 3 shows that Au at the interstitial site
201 causes the pyrite to be spin-polarized (the solid line indicates the spin-up state (alpha),
202 and the dashed line indicates the spin-down state (beta)) at a certain As content. The
203 spin density of states (DOS) is mainly derived from the Fe 3d state, and the magnetic
204 moments are 0.33 hbar.

205 The changes in the electronic structures can be clearly observed from the DOS of
206 the pyrite, as shown in Fig. 4. It is shown that the DOS of $\text{Fe}_{32}\text{S}_{62}\text{AsAu}$ (Au and As
207 substituting for S atoms) is very similar to that of $\text{Fe}_{32}\text{S}_{64}$, whereas the DOS of
208 $\text{Fe}_{32}\text{S}_{64-x}\text{As}_x\text{Au}$ ($x=1-4$) are significantly shifted to a low-energy value, and there are
209 apparent DOS between the valence band and conduction band. It is noted that there is
210 DOS at the Fermi energy level for pure pyrite ($\text{Fe}_{32}\text{S}_{64}$) which is insulating material.
211 One of the reasons for this result is that the Fermi energy level is underestimated in
212 the DOS calculation. In addition, the setting of the Gaussian broadening of the
213 eigenvalues (smearing width) is also very important for the calculation.

214 By analyzing the Mulliken bond population, it has been shown that antibonding
215 interactions existed between the Au-Fe atoms and Au-As atoms. This interaction can
216 be further analyzed by plotting the density of states of the atoms, where the
217 antibonding interactions of the s, p and d orbitals between atoms can be clearly shown.
218 Fig. 5 presents the s, p and d orbitals of Au, As and Fe at energies ranging from -2 to 2
219 eV. It can be clearly seen that strong hybridizations occur between the 6p and 5d

220 orbitals of the Au atoms. In addition, strong interactions are found between the Fe 3d
221 and Au 6p orbitals and between the Au 5d and As 4p orbitals.

222 **Acknowledgments**

223 The authors are grateful for the financial support provided by the Open Fund of
224 the State Key Laboratory of Comprehensive Utilization of Low-Grade Refractory
225 Gold Ores (Zijin Mining Group Co., Ltd) and by the National Natural Science
226 Foundation of China (NSFC. 51164001). They are also grateful for the support from
227 the Shanghai Supercomputer Center.

228 **References:**

229 Abraitis P.K., Patrick R.A.D, and Vaughan D.J. (2004) Variations in the
230 compositional, textural and electrical properties of natural pyrite: a review.
231 International Journal of Mineral Processing, 74, 41–59.

232 Arehart G.B., Eldridge C.S., Chryssoulis S.L., and Kesler S.E. (1993) Ion
233 microprobe determination of sulfur isotope variations in iron sulfides from the
234 Post/Betze sediment hosted disseminated gold deposit, Nevada, USA.
235 Geochimica et Cosmochimica Acta, 57, 1505–1519.

236 Blanchard M., Alfredsson M., Brodholt J., Wright K., and Catlow C.R.A. (2007)
237 Arsenic incorporation into FeS₂ pyrite and its influence on dissolution: A DFT
238 study, Geochimica et Cosmochimica Acta, 71, 624–630.

239 Cocula V., Starrost F., Watson S. C., and Carter E.A. (2003) Spin-dependent
240 pseudopotentials in the solid-state environment: Applications to ferromagnetic
241 and antiferromagnetic metals. Journal of Chemical Physics, 119, 7659-7671.

242 .Cook N.J., and Chryssoulis S.L. (1990) Concentrations of invisible gold in the

- 243 common sulfides. *Canadian Mineralogist*, 28, 1–16.
- 244 Fleet M.E., Chryssoulis S.L., Maclean P.J., Davidson R., and Weisener C.G. (1993)
245 Arsenian pyrite from gold deposits—Au and vAs distribution investigated by
246 SIMS and EMP, and colour staining and surface oxidation by XPS and LIMS.
247 *Canadian Mineralogist*, 31, 1–17.
- 248 Hohenberg P., and Kohn W. (1964) Inhomogeneous electron gas. *Physical Review*,
249 136, B864-B871.
- 250 Kohn W., and Sham L.J. (1965) Self-consistent equations including exchange and
251 correlation effects. 140, A1133–A1138.
- 252 Monkhorst H.J., and Pack J.D. (1976) Special points for Brillouin-zone integrations.
253 *Physical Review B*, 13, 5188–5192.
- 254 Nishidate K., Yoshizawa M., and Hasegawa M. (2008) Energetics of Mg and B
255 adsorption on polar zinc oxide surfaces from first principles. *Physical Review B*,
256 77, 035330-1–035330-6.
- 257 Pack J.D., and Monkhorst H.J. (1977) "Special points for Brillouin-zone integrations"
258 — a reply. *Physical review B*, 16, 1748–1749.
- 259 Perdew J.P., Chevary J.A., Vosko S.H.K., Jackson K.A., Pederson M.R., Singh D.J.,
260 and Fiolhais C. (1992) Atoms, molecules, solids, and surfaces: Applications of
261 the generalized gradient approximation for exchange and correlation. *Physical*
262 *Review B*, 46, 6671–6687.
- 263 Prince K.C., Matteucci M., Kuepper K., Chiuzbaian S.G., Barkowski S., and
264 Neumann M. (2005) Core-level spectroscopic study of FeO and FeS₂. *Physical*

- 265 Review B, 71 085102-1–085102-9.
- 266 Reich M., Palenik C. S., Utsunomiya S., Becker U., Stixrude L., Kesler S. E., and
267 Ewing R. C. (2003) Solubility limit of gold in arsenian pyrite from Carlin-type
268 and epithermal deposits: EMPA, SIMS, HRTEM and quantum mechanical
269 constraints. Geological Society of America. Abstracts with Programs, 35, 358.
- 270 Reich M., Kesler S. E., Utsunomiya S., Palenik C. S., Chryssoulis S.L., and Ewing R.
271 C. (2005) Solubility of gold in arsenian pyrite. *Geochimica et Cosmochimica*
272 *Acta*, 69, 2781–2796.
- 273 Savage K.S., Tingle T.N., O’Day P.A., Waychunas G.A., and Bird D. K. (2000)
274 Arsenic speciation in pyrite and secondary weathering phases, Mother Lode gold
275 district, Tuolumne County, California. *Applied Geochemistry*, 15, 1219–1244.
- 276 Schlegel A., and Wachter P. (1976) Optical properties, phonons and electronic
277 structure of iron pyrite (FeS₂). *Journal of Physics C: Solid State Physics*, 9,
278 3363-3369.
- 279 Segall M.D., Shah R., Pickardk C.J., and Payne M.C. (1996) Population analysis of
280 plane-wave electronic structure calculations of bulk materials. *Physical review B*,
281 54, 16317–16320.
- 282 Simon G., Huang H., Penner-Hahn J.E., Kesler S.E., and Kao L.S. (1999) Oxidation
283 state of gold and arsenic in gold-bearing arsenian pyrite. *American Mineralogist*,
284 84, 1071–1079.
- 285 Vanderbilt D. (1990) Soft self-consistent pseudopotentials in a generalized eigenvalue
286 formalism. *Physical Review B*, 41, 7892–7895.

287 Von Barth U., and Hedin L.A. (1972) Local exchange-correlation potential for the
288 spin polarized case. *Journal of Physics C*, 5, 1629-1642.

289 Vosko S.J., Wilk L., and Nusair M. (1980) Accurate spin-dependent electron liquid
290 correlation energies for local spin density calculations: A critical analysis.
291 *Canadian Journal of Physics*, 58, 1200-1211.

292 Wells J.D., and Mullens T.E. (1973) Gold-bearing arsenian pyrite determined by
293 microprobe analysis, Cortez and Carlin gold mines, Nevada. *Economic Geology*,
294 68, 187–201.

295 **Figure captions**

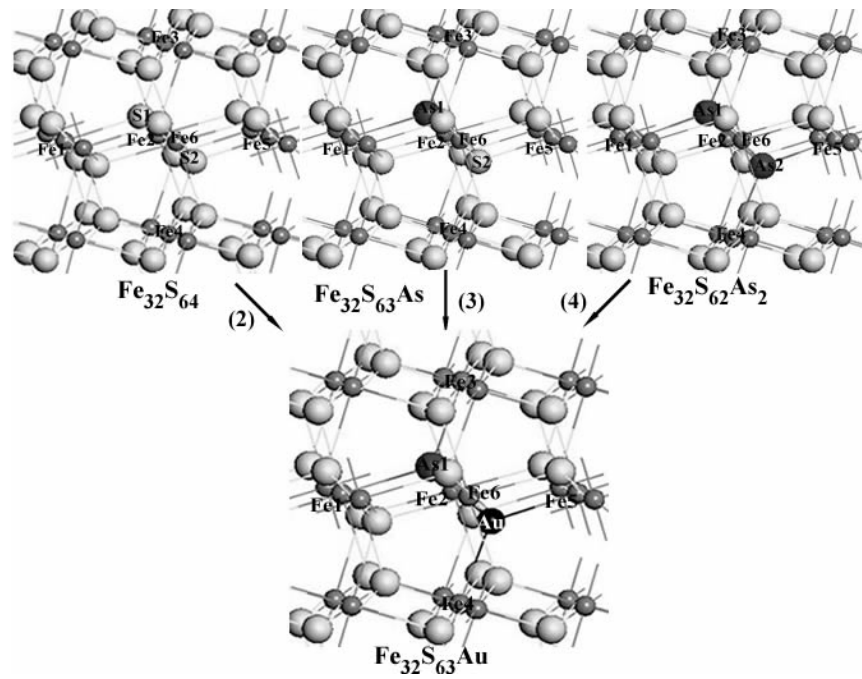
296 **FIGURE 1.** Reacting processes of (2)-(4). Au is incorporated into the S site under
297 different As mass concentrations.

298 **FIGURE 2.** Reacting processes of (5)-(9). Au is incorporated at interstitial site in
299 pyrite under different As mass concentrations.

300 **FIGURE 3.** Band structures of perfect and Au- and As-bearing pyrites. The solid line
301 indicates the spin-up (alpha) state, and the dashed line indicates the spin-down (beta)
302 state. The zero of the energy has been set at the Fermi level, E_F .

303 **FIGURE 4.** Density of states (DOS) of the perfect pyrite and that of Au- and
304 As-bearing pyrite. The zero of the energy has been set at the Fermi level, E_F .

305 **FIGURE 5.** DOS of Fe, Au and As atoms in pyrite. The zero of the energy has been
306 set at the Fermi level, E_F .



307
308

FIGURE 1

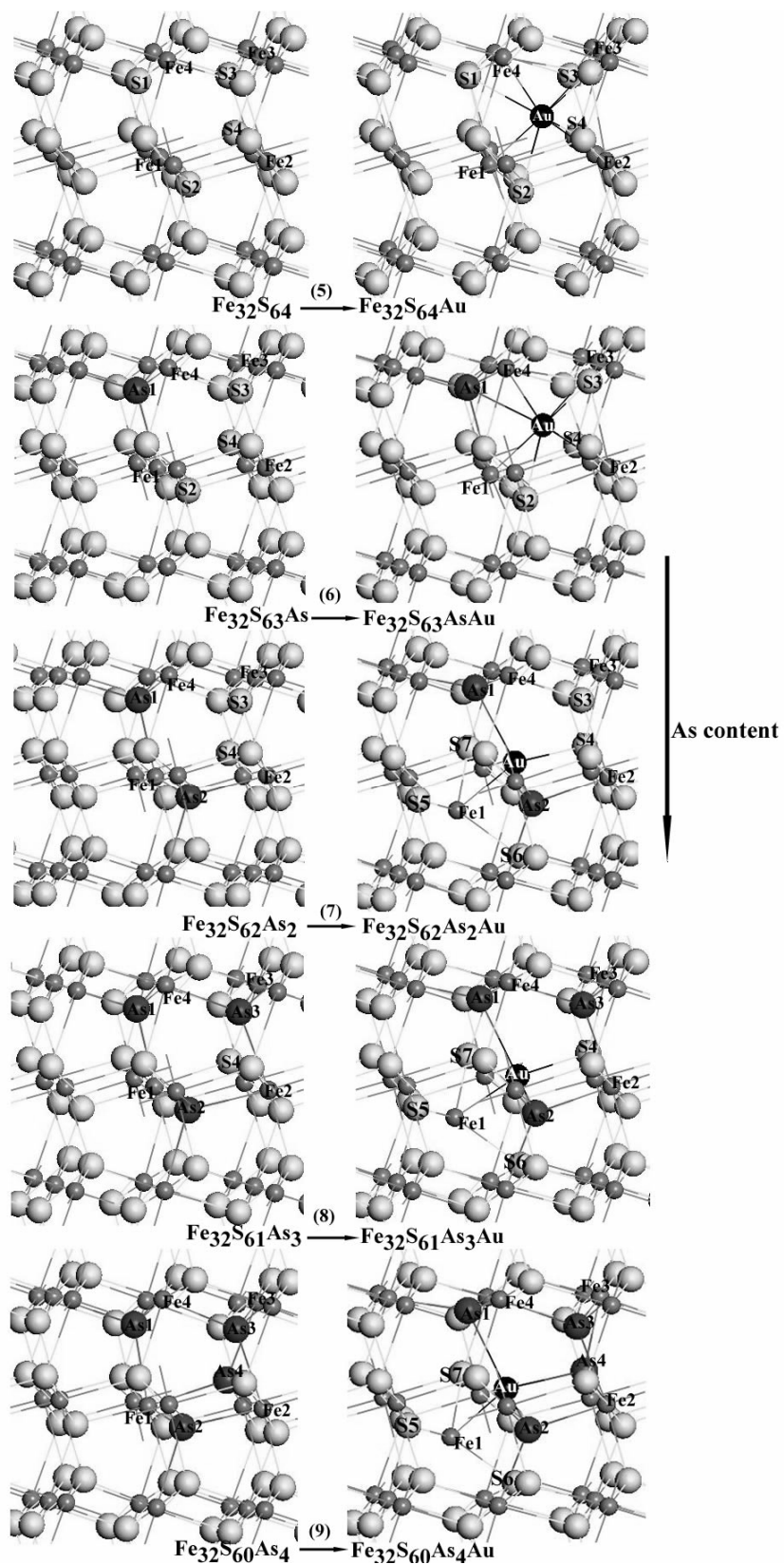
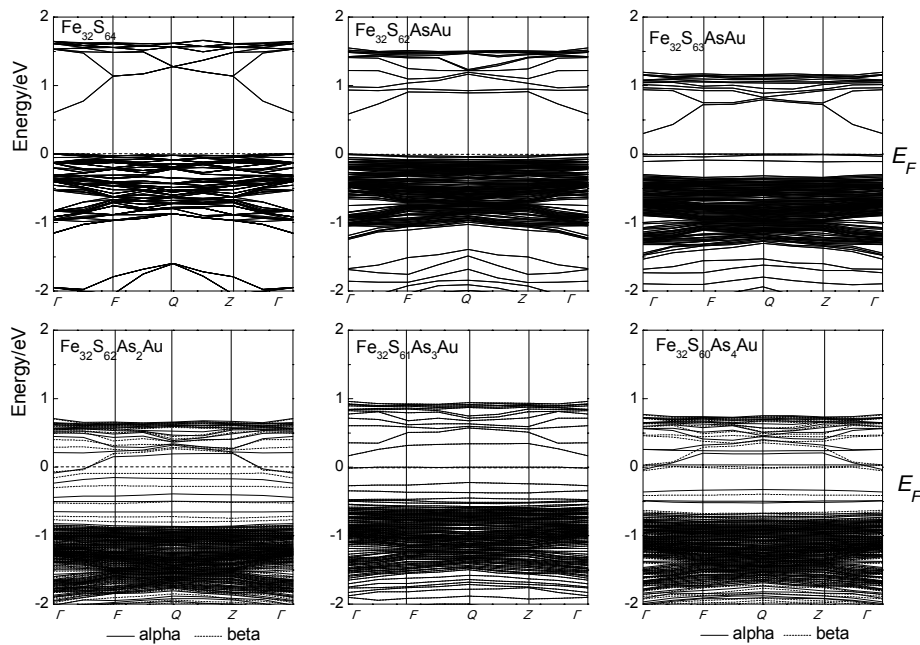


FIGURE 2

309

310

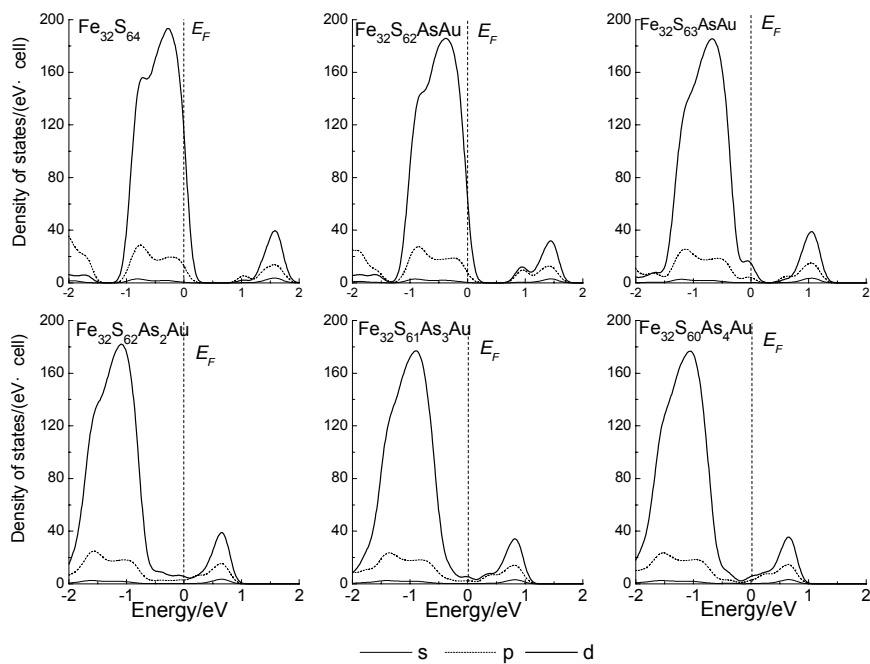
311



312

313

FIGURE 3

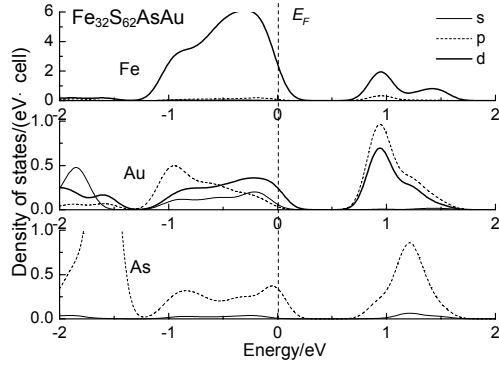


314

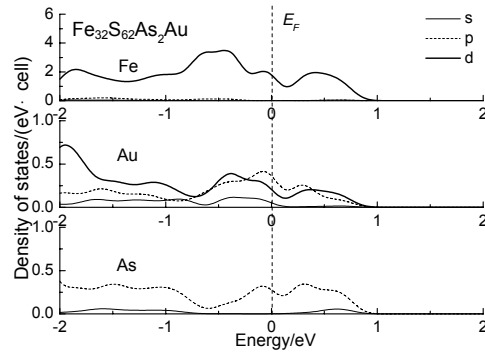
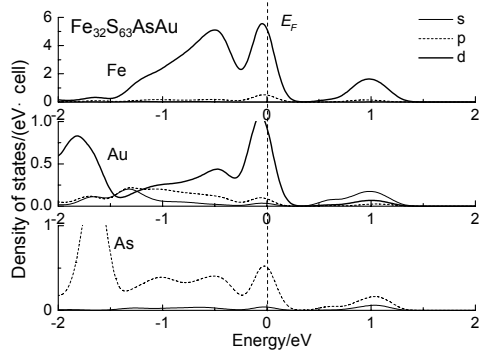
315

FIGURE 4

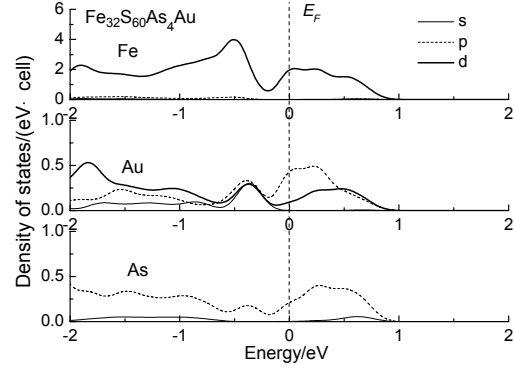
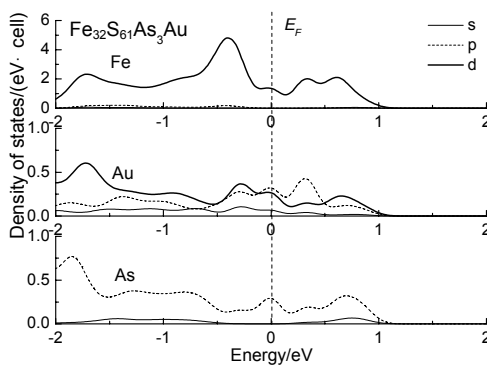
316



317



318



319

FIGURE 5

320

TABLE 1 Formation energies for reactions (1)-(9)

Reactions	Formation energy /
(1)	+10.97
(2)	+4.62
(3)	+3.96
(4)	+2.86
(5)	+5.89
(6)	+4.67
(7)	+2.00
(8)	+1.33
(9)	+0.67

Note: The standard deviation value is 0.005 eV.

TABLE 2 Lattice structure of pyrite containing Au and As

Species	Cell lengths /Å			Angles /degree		
	a	b	c	α	β	γ
Fe ₃₂ S ₆₄	10.836	10.836	10.836	90.00	90.00	90.00
Fe ₃₂ S ₆₂ AsAu	10.873	10.873	10.873	89.84	90.22	89.80
Fe ₃₂ S ₆₃ AsAu	10.958	10.949	10.955	89.72	89.68	89.86
Fe ₃₂ S ₆₂ As ₂ Au	10.979	10.947	10.950	89.73	89.76	89.70
Fe ₃₂ S ₆₁ As ₃ Au	10.984	10.945	10.962	89.69	89.83	89.64
Fe ₃₂ S ₆₀ As ₄ Au	10.975	10.975	10.972	89.65	89.64	89.67

Note: The standard deviation value for cell length is 0.002 Å and for angle is 0.01 degree.

TABLE 3 Mulliken population of bond in pyrite

	Species	Bond	Length /Å	Population
Substituting Au	Fe ₃₂ S ₆₂ AsAu	As1-Au	2.426	-0.12
		(Fe4, Fe5, Fe6)-Au	2.425	-0.40
Interstitial Au	Fe ₃₂ S ₆₃ AsAu	As1-Au	2.381	-1.08
		(Fe1, Fe2, Fe3, Fe4)-Au	2.380—2.666	-0.82—-1.26
	Fe ₃₂ S ₆₂ As ₂ Au	(As1, As2)-Au	2.408	-0.05
		Fe1-Au	2.419	-0.30
	Fe ₃₂ S ₆₁ As ₃ Au	(As1, As2)-Au	2.428	-0.03
		Fe1-Au	2.408	-0.22
	Fe ₃₂ S ₆₀ As ₄ Au	(As1, As2, As4)-Au	2.455	-0.05
		Fe1-Au	2.393	-0.05

Note: The standard deviation value of bond length is 0.002 Å..